

See discussions, stats, and author profiles for this publication at: <https://www.researchgate.net/publication/261707701>

# Enhanced Water Splitting Efficiency Through Selective Surface State Removal

ARTICLE *in* JOURNAL OF PHYSICAL CHEMISTRY LETTERS · APRIL 2014

Impact Factor: 7.46 · DOI: 10.1021/jz500535a

---

CITATIONS

25

---

READS

131

## 2 AUTHORS:



Omid Zandi

University of Texas at Austin

14 PUBLICATIONS 221 CITATIONS

SEE PROFILE



Thomas William Hamann

Michigan State University

52 PUBLICATIONS 2,202 CITATIONS

SEE PROFILE

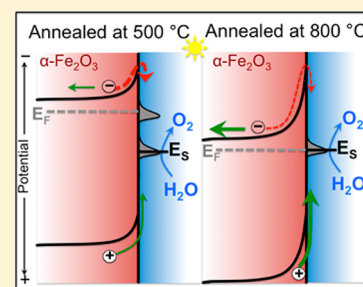
# Enhanced Water Splitting Efficiency Through Selective Surface State Removal

Omid Zandi and Thomas W. Hamann\*

Department of Chemistry, Michigan State University, East Lansing, Michigan 48824-1322, United States

**S** Supporting Information

**ABSTRACT:** Hematite ( $\alpha\text{-Fe}_2\text{O}_3$ ) thin film electrodes prepared by atomic layer deposition (ALD) were employed to photocatalytically oxidize water under 1 sun illumination. It was shown that annealing at 800 °C substantially improves the water oxidation efficiency of the ultrathin film hematite electrodes. The effect of high temperature treatment is shown to remove one of two surface states identified, which reduces recombination and Fermi level pinning. Further modification with Co–Pi water oxidation catalyst resulted in unprecedented photocurrent onset potential of  $\sim 0.6$  V versus reversible hydrogen electrode (RHE; slightly positive of the flat band potential).



**SECTION:** Energy Conversion and Storage; Energy and Charge Transport

Solar-driven water splitting offers the possibility of generating an essentially unlimited supply of clean-burning hydrogen fuel using sunlight and water.<sup>1–4</sup> Hematite photoanodes have been studied extensively to carry the water oxidation half reaction of the overall water splitting process during the last three decades.<sup>5–7</sup> Being an earth abundant material along with chemical stability and substantial visible light absorption put hematite among the most attractive semiconductor materials for this purpose.<sup>3,6</sup> Despite the extensive research in the field, efficient water oxidation with hematite electrodes has not been achieved mainly due to an intrinsically short minority carrier (hole) collection length.<sup>5,8,9</sup> We note that bulk modification, e.g., doping,<sup>10–12</sup> nanostructuring,<sup>8,13–15</sup> and substrate modification<sup>16,17</sup> can improve the efficiency by enhancing the charge separation in the bulk and thereby increase the flux of holes reaching the electrode surface.<sup>8,18</sup>

While a short hole collection length limits the flux of holes reaching the electrode surface, recombination of the surface holes with conduction band electrons is another major factor limiting the water oxidation efficiency.<sup>3,19–22</sup> It is generally only at very positive biases, where increased band bending reduces the electron concentration at the electrode surface, that water oxidation can outcompete recombination and produce a steady-state photocurrent.<sup>20,22</sup> Thus, surface state recombination is reflected in a high photocurrent onset potential of around 1.1–1.2 V versus reversible hydrogen electrode (RHE) for the majority of reported bare hematite electrodes. A very straightforward way to quantify the water oxidation efficiency loss due to surface recombination is to compare the photocurrent density versus applied voltage ( $J$ – $V$ ) behavior of electrodes in contact with  $\text{H}_2\text{O}$  and a hole scavenger such as  $[\text{Fe}(\text{CN})_6]^{4-}$  or  $\text{H}_2\text{O}_2$ .<sup>23,24</sup> Previous studies showed that hole collection efficiency by a hole scavenger is essentially unity.

Therefore, any differences in the  $J$ – $V$  behavior for electrodes in contact with an aqueous electrolyte, with and without a good hole scavenger, can be unambiguously attributed to surface state recombination. Using such an approach, it was shown that surface recombination is responsible for the loss of  $\sim 600$  mV of photovoltage.<sup>23,24</sup> Strategies targeting the photocurrent onset are mainly based on modifications of the electrode surface. In fact, the state-of-the-art devices have produced promising results by applying efficient water oxidation catalyst systems such as Co–Pi.<sup>25–27</sup> For this system, the photovoltage was improved by  $\sim 0.25$  V, which we attributed to better charge separation, thus reducing surface state recombination.<sup>25</sup> Recently a photocurrent onset as low as  $\sim 0.62$  V vs RHE was reported by Du et al. for thin film hematite electrodes modified with a  $\text{NiFeO}_x$  catalyst.<sup>28</sup> Numerous examples of an onset potential shift upon incorporation of water oxidation catalysts, and oxide overlayers all indicate the importance of surface properties on the water oxidation performance of hematite electrodes. Here we show that a water oxidation onset potential as low as  $\sim 0.7$  V vs RHE is achievable for a bare hematite electrode by annealing out deleterious surface states. Further modification with Co–Pi reduces the onset potential to produce the highest reported photovoltage to date.

Ultrathin 20 nm films of hematite were deposited on  $\text{Ga}_2\text{O}_3$  coated F:SnO<sub>2</sub> (FTO) substrates via 300 atomic layer deposition cycles using a previously established method.<sup>11</sup> We have shown that 2 nm  $\text{Ga}_2\text{O}_3$  underlayer improves the water oxidation performance and reproducibility of ultrathin hematite films (unpublished results). Detailed experimental conditions are provided in the Supporting Information (SI). We note that

**Received:** March 15, 2014

**Accepted:** April 10, 2014

such ultrathin films can ultimately be applied to high surface area nanostructured templates to increase light absorption and produce overall efficient water splitting.<sup>15,29</sup> The hematite films were first annealed by heating to 500 °C at a rate of 17 °C/min, sintered at 500 °C for 30 min, and allowed to cool to room temperature over 2 h. Electrodes were the further annealed at 800 °C for 4 min and transferred to room temperature. Control experiments showed that annealing at 800 °C for 4 min does not have any measurable effect on the conductivity of FTO substrates, in agreement with previous reports.<sup>27</sup> Figure 1

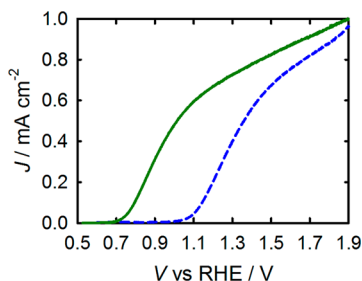


**Figure 1.**  $J$ – $V$  curves of 20 nm hematite electrodes annealed at 500 °C (dashed blue) and 800 °C (solid green) under  $\text{H}_2\text{O}$  oxidation conditions at pH 13.6 and 1 sun illumination. Dark  $J$ – $V$  curves are provided in the SI.

shows  $J$ – $V$  curves of typical bare hematite films annealed at 500 and 800 °C. The high temperature annealing dramatically improves the photocurrent onset potential, with a cathodic shift of the  $J$ – $V$  curve in excess of 300 mV. Control electrodes without a  $\text{Ga}_2\text{O}_3$  underlayer that were annealed at 800 °C exhibit a more modest cathodic shift of ~100 mV, indicating a synergistic effect of the  $\text{Ga}_2\text{O}_3$  underlayer and high temperature annealing (Figure 6S in the SI). Uncovering the details of this synergy is the subject of ongoing investigation in our laboratory. We note that a cathodic shift of the  $\text{H}_2\text{O}$  oxidation onset potential upon annealing at 800 °C was also observed by Sivula et al.,<sup>13</sup> and Ling et al.<sup>30</sup> More recently, Kim et al. reported the best overall water splitting performance of hematite electrodes, which were annealed at 800 °C; however, the effect of annealing temperature was not explored.<sup>27</sup>

The cathodic shift in the  $\text{H}_2\text{O}$  oxidation photocurrent onset is generally attributed to improved water oxidation efficiency through suppression of surface electron/hole recombination. Sivula et al. attributed their improved photocurrent onset to bulk doping by the substrate, however, not a surface effect. Intentional doping has been shown to make modest (at best) improvements to the photocurrent onset potential, and cannot account for the dramatic decrease in photocurrent onset as discussed below.<sup>31–33</sup> In order to separate any improvement due to modification of the bulk film from the surface effects,  $J$ – $V$  measurements were performed in the presence of  $\text{H}_2\text{O}_2$  and compared to that of  $\text{H}_2\text{O}$  oxidation. The  $J$ – $V$  responses for both electrodes in contact with  $\text{H}_2\text{O}_2$  (top panel of Figure 2) are nominally identical, with no significant difference in the photocurrent or photovoltage. Therefore, the  $J$ – $V$  difference observed between electrodes annealed at 500 and 800 °C under water oxidation conditions is strictly a consequence of surface effects. We previously showed that when a good hole scavenger is present, the photocurrent onset potential coincides with the flat band potential.<sup>34</sup> Since the photocurrent onset is the same for electrodes annealed at 500 and 800 °C in contact with

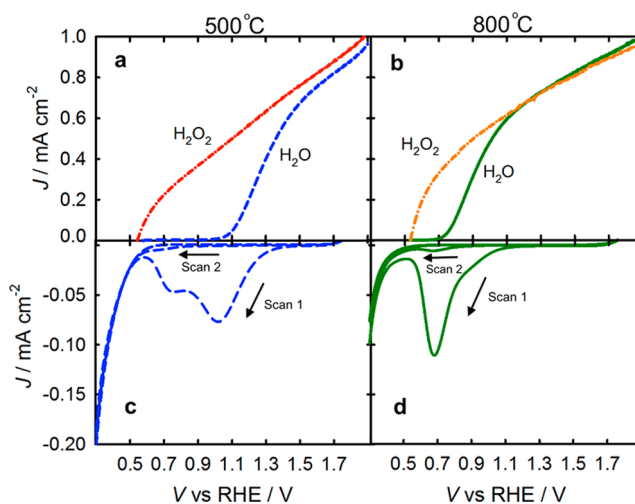


**Figure 2.**  $J$ – $V$  curves under  $\text{H}_2\text{O}$  and  $\text{H}_2\text{O}_2$  oxidation conditions for hematite electrodes annealed at 500 °C (a) and 800 °C (b). CV curves scanned at 1 V/s in the dark of the electrodes annealed at 500 °C (c) and 800 °C (d).

$\text{H}_2\text{O}_2$ , the band positions are unaffected by the annealing temperature.

The role of surface states in the photocatalytic water oxidation reaction with hematite electrodes prepared by atomic layer deposition (ALD) has already been investigated in detail, including the pH and light intensity dependence.<sup>19,20</sup> It was shown that the water oxidation onset is associated with the accumulation of photogenerated holes at the electrode surface which manifests as a capacitance.<sup>20</sup> This surface state capacitance has a peak around the onset of water oxidation that can be observed through electrochemical impedance (EIS) measurements, photocurrent transients, and cyclic voltammetry (CV) measurements.<sup>19,20</sup> In addition to these surface states, another set of states was observed in the CV measurements at more negative potentials (around the flat band potential). These states showed a similar transient behavior during anodic oxidation, i.e., only observed at relatively high scan rates.<sup>20</sup>

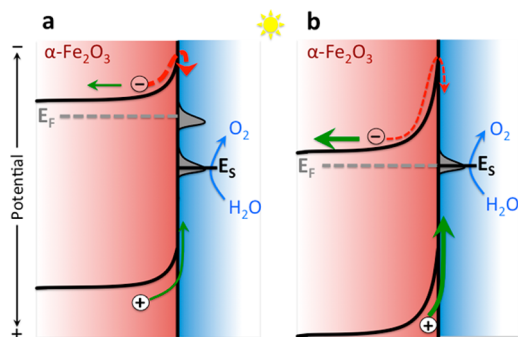
In order to examine the effect of high temperature annealing on the surface states properties, CV measurements were carried out of the electrodes annealed at 500 and 800 °C. For this purpose, electrodes were held at 2 V vs RHE under 1 sun illumination for 60 s (in order to photoelectrochemically oxidize the surface states) followed by measuring the cathodic current in the dark as the potential is scanned negatively at 1 V/s (Figure 2c,d). A plot of CV curves measured as a function of scan rate is provided in the SI (Figure 2S). For the control hematite electrode (annealed at 500 °C) on the first scan two peaks in current appear at around 1.1 and 0.65 V vs RHE. On the second cycle, both of these peaks are gone due to the transient nature of the oxidized states, in agreement with the previous work.<sup>20</sup>

For the electrodes annealed at 800 °C, only one peak was observed, which coincides with the  $\text{H}_2\text{O}$  oxidation onset potential. The first cathodic peak, which always appears at potentials around the photocurrent onset, has been assigned to the reduction of oxidized surface species ( $\text{H}_2\text{O}$  oxidation intermediates).<sup>20</sup> Therefore, we attribute the first cathodic peak (~1.1 V for control electrode and ~0.7 V for the electrodes annealed at 800 °C) to the same effect. The absence of the second peak at ~0.65 V for the electrodes annealed at 800 °C, clearly indicates the passivation of this set of surface states with

an energy close the flat band (i.e.,  $\sim 0.52$  V vs RHE) upon annealing. This finding is consistent with a recent report by Kronawitter et al., who utilized soft X-ray absorption spectroscopy to show that high-temperature annealing can remove oxygen p-hybridized states located just below the conduction band minimum.<sup>35</sup> The existence of a surface states at this energy is also consistent with observations by others through transient absorption spectroscopy measurements.<sup>21,36</sup>

Surface states with an energy above the charge neutrality level can potentially pin the Fermi level of an n-type semiconductor, which gives rise to a fixed barrier height.<sup>37,38</sup> The density and energy distribution of surface states, therefore, dictates the extent of band bending (barrier height) at the interface. The shallow states identified herein can thus pin the Fermi level and limit the extent of band bending at the hematite/solution interface, which controls electron–hole separation. This situation is depicted in Scheme 1. Indeed,

**Scheme 1. Simplified Band Diagram of Hematite Electrodes under Conditions with (a) and without (b) Fermi Level Pinning by the Sub-Conduction Band Surface States**



we previously showed Fermi level pinning can account for  $\sim 200$  mV shift in the  $J$ – $V$  curves under water oxidation conditions compared to when a fast hole collector was present.<sup>20</sup> The  $J$ – $V$  curves of the hematite electrode annealed in  $500^\circ\text{C}$  in contact with  $\text{H}_2\text{O}$  and  $\text{H}_2\text{O}_2$  (Figure 2a) do not overlap exactly at positive potentials; the  $\text{H}_2\text{O}_2$  electrolyte always produces somewhat higher photocurrent at a given applied potential compared to water oxidation conditions.<sup>23,24</sup> This discrepancy can be attributed to the extra potential needed to compensate for Fermi level pinning during water oxidation. As seen in Figure 2b, this is not the case for the electrode annealed at  $800^\circ\text{C}$ . We therefore attribute part of the increased photovoltage upon annealing at  $800^\circ\text{C}$  to the mitigation of Fermi level pinning at the hematite/electrolyte interface by passivating the set of surface states right below the conduction band. The remainder of the increased photovoltage achieved through high temperature annealing is due to the decreased surface state recombination.

While a remarkable improvement in the photovoltage has been achieved (from Figure 2b), the onset of  $\text{H}_2\text{O}$  oxidation is still  $\sim 200$  mV more positive compared to  $\text{H}_2\text{O}_2$  oxidation (i.e., the onset potential is  $\sim 200$  mV positive of the flat band potential). This discrepancy can be clearly seen in the chopped light  $J$ – $V$  curve shown in Figure 3a. At potentials just positive of the flat band, even though hole accumulation at the surface occurs (transient peak in current), the recombination rate is too high to allow any steady state faradaic current. Assuming the same flux of holes from the bulk for electrodes in contact with  $\text{H}_2\text{O}$  and  $\text{H}_2\text{O}_2$ , the difference in the  $J$ – $V$  responses shown in

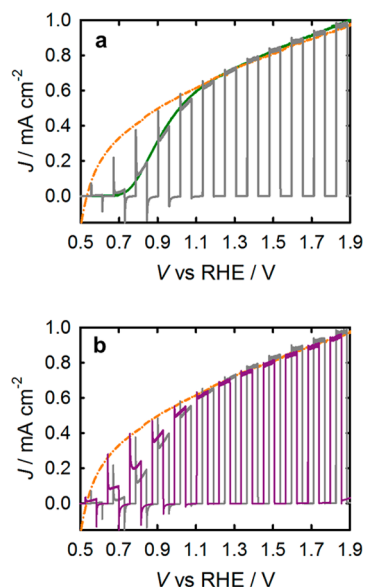


**Figure 3.** (a)  $J$ – $V$  curves of a hematite electrode annealed at  $800^\circ\text{C}$  in contact with  $\text{H}_2\text{O}$  under chopped (solid gray) and continuous (solid green) 1 sun illumination. (b) Chopped light  $J$ – $V$  curves of bare (solid gray) and Co–Pi-coated (solid purple) hematite electrodes in contact with  $\text{H}_2\text{O}$  under 1 sun illumination. The  $J$ – $V$  curve of the bare electrode under  $\text{H}_2\text{O}_2$  oxidation (dash dotted orange) is also shown for comparison.

Figure 3a can be explained in terms of the slow kinetics of  $\text{H}_2\text{O}$  oxidation not being able to compete with recombination at these potentials; however, the fast kinetics of  $\text{H}_2\text{O}_2$  oxidation can. If this is indeed the case, modification of the hematite surface with a water oxidation catalyst should push the onset potential toward that of  $\text{H}_2\text{O}_2$  oxidation. The Co–Pi catalyst has been shown to enhance the water oxidation efficiency by transferring holes to the Co–Pi instead of surface states, which alleviates Fermi level pinning and diminishes surface state recombination.<sup>25,26,39</sup> Therefore, hematite electrodes annealed at  $800^\circ\text{C}$  were further coated with Co–Pi via photoelectrodeposition following the procedure reported previously.<sup>25,26</sup>  $J$ – $V$  curves of a hematite electrode coated with Co–Pi is shown in Figure 3b. The Co–Pi modification resulted in an additional  $\sim 100$  mV shift of the onset potential with a concomitant photocurrent increase at lower biases. The photocurrent and photovoltage are still less than that of  $\text{H}_2\text{O}_2$  oxidation at these low applied biases, which indicates that the rate of surface recombination is still relevant for  $\text{H}_2\text{O}$  oxidation on high temperature annealed surfaces with a Co–Pi catalyst, however it is significantly reduced. Hematite electrodes annealed at  $500^\circ\text{C}$  that were coated with Co–Pi exhibited analogous behavior as previously reported (Figure 4S in the SI).<sup>25</sup>

The stability of hematite/Co–Pi photoanode systems under  $\text{H}_2\text{O}$  oxidation conditions is well established.<sup>25–27</sup> However, to further confirm the stability and reproducibility of the hematite electrodes annealed at  $800^\circ\text{C}$ , six different electrodes from different ALD batches were annealed at  $800^\circ\text{C}$  and tested under water oxidation conditions. Reproducible stable  $J$ – $V$ , CV, and steady state photocurrent were measured in the presence/absence of dissolved  $\text{O}_2$  and  $\text{N}_2$ , further confirming the reproducibility and stability of our photoanode system (see Figure 3S).



In summary, it was demonstrated that the photovoltage of H<sub>2</sub>O oxidation on hematite electrodes can be significantly improved upon annealing at 800 °C. CV measurements revealed that a set of surface states with an energy of slightly below the flat band potential are eliminated upon annealing at 800 °C. The performance improvement was therefore attributed to the mitigation of Fermi level pinning by these states and a reduction of surface state recombination. Even with the high temperature annealing, there is an additional surface state that coincides with the water oxidation onset potential that we attributed to water oxidation intermediates. The fact that this state remains prominent, and coincides with the photocurrent onset, following the high temperature annealing, supports this assignment. These results are significant as it reconciles the interpretation of surface states throughout the literature as we clearly show that there are two very distinct states, one set that is problematic and another that is inherent in the water oxidation process. Moreover, a route to improve the photovoltage by selectively eliminating the deleterious surface states was demonstrated. We note that it is unlikely that the photocurrent onset would be negative of the flat band potential, and we have shown that the combination of high temperature annealing and the addition of a water oxidation catalyst produce an onset potential only 100 mV more positive of the flat band, thus very little further improvement is probable.

## ■ ASSOCIATED CONTENT

### ● Supporting Information

Detailed experimental conditions, dark *J*–*V* curves, *J*–*V* curves of electrodes annealed at 500 °C and modified with Co-Pi, scan rate dependence of the CV measurements, stability tests, and SEM images can be found in the SI. This material is available free of charge via the Internet at <http://pubs.acs.org>.

## ■ AUTHOR INFORMATION

### Corresponding Author

\*E-mail: [hamann@chemistry.msu.edu](mailto:hamann@chemistry.msu.edu).

### Notes

The authors declare no competing financial interest.

## ■ ACKNOWLEDGMENTS

T.W.H. is grateful to the National Science Foundation (CHE-1150378) for support of this research.

## ■ REFERENCES

- (1) Lewis, N. S. Toward Cost-Effective Solar Energy Use. *Science* **2007**, *315*, 798–801.
- (2) Walter, M. G.; Warren, E. L.; McKone, J. R.; Boettcher, S. W.; Mi, Q.; Santori, E. A.; Lewis, N. S. Solar Water Splitting Cells. *Chem. Rev.* **2010**, *110*, 6446–6473.
- (3) Young, K. M. H.; Klahr, B. M.; Zandi, O.; Hamann, T. W. Photocatalytic Water Oxidation with Hematite Electrodes. *Catal. Sci. Technol.* **2013**, *3*, 1660–1671.
- (4) Sivula, K. *Photoelectrochemical Hydrogen Production*; van de Krol, R., Grätzel, M., Eds.; Electronic Materials: Science & Technology; Springer: Boston, MA, 2012; Vol. 102.
- (5) Hamann, T. W. Splitting Water with Rust: Hematite Photoelectrochemistry. *Dalton Trans.* **2012**, *41*, 7830–7834.
- (6) Sivula, K.; Le Formal, F.; Grätzel, M. Solar Water Splitting: Progress Using Hematite ( $\alpha$ -Fe<sub>2</sub>O<sub>3</sub>) Photoelectrodes. *ChemSusChem* **2011**, *4*, 432–449.
- (7) Katz, M. J.; Riha, S. C.; Jeong, N. C.; Martinson, A. B. F.; Farha, O. K.; Hupp, J. T. Toward Solar Fuels: Water Splitting with Sunlight and “Rust”? *Coord. Chem. Rev.* **2012**, *256*, 2521–2529.
- (8) Kay, A.; Cesar, I.; Grätzel, M. New Benchmark for Water Photooxidation by Nanostructured  $\alpha$ -Fe<sub>2</sub>O<sub>3</sub> Films. *J. Am. Chem. Soc.* **2006**, *128*, 15714–15721.
- (9) Zhao, B.; Kaspar, T. C.; Droubay, T. C.; McCloy, J.; Bowden, M. E.; Shutthanandan, V.; Heald, S. M.; Chambers, S. A. Electrical Transport Properties of Ti-Doped Fe<sub>2</sub>O<sub>3</sub>(0001) Epitaxial Films. *Phys. Rev. B* **2011**, *84*, 245325.
- (10) Cesar, I.; Sivula, K.; Kay, A. Influence of Feature Size, Film Thickness, and Silicon Doping on the Performance of Nanostructured Hematite Photoanodes for Solar Water Splitting. *J. Phys. Chem. C* **2009**, *113*, 772–782.
- (11) Zandi, O.; Klahr, B.; Hamann, T. Highly Photoactive Ti-Doped  $\alpha$ -Fe<sub>2</sub>O<sub>3</sub> Thin Film Electrodes; Resurrection of the Dead Layer. *Energy Environ. Sci.* **2012**, *5*, 634–642.
- (12) Hu, Y.; Kleiman-shwarsstein, A.; Forman, A. J.; Hazen, D.; Park, J.; McFarland, E. W.; Barbara, S. Pt-Doped  $\alpha$ -Fe<sub>2</sub>O<sub>3</sub> Thin Films Active for Photoelectrochemical Water Splitting. *Chem. Mater.* **2008**, *20*, 3803–3805.
- (13) Sivula, K.; Zboril, R.; Le Formal, F.; Robert, R.; Weidenkaff, A.; Tucek, J.; Frydrych, J.; Grätzel, M. Photoelectrochemical Water Splitting with Mesoporous Hematite Prepared by a Solution-Based Colloidal Approach. *J. Am. Chem. Soc.* **2010**, *132*, 7436–7444.
- (14) Mayer, M. T.; Lin, Y.; Yuan, G.; Wang, D. Forming Heterojunctions at the Nanoscale for Improved Photoelectrochemical Water Splitting by Semiconductor Materials: Case Studies on Hematite. *Acc. Chem. Res.* **2013**, *46*, 1558–1566.
- (15) Riha, S. C.; Devries Vermeer, M. J.; Pellin, M. J.; Hupp, J. T.; Martinson, A. B. F. Hematite-Based Photo-Oxidation of Water Using Transparent Distributed Current Collectors. *ACS Appl. Mater. Interfaces* **2013**, *5*, 360–367.
- (16) Hisatomi, T.; Brillet, J.; Cornuz, M.; Le Formal, F.; Tétreault, N.; Sivula, K.; Grätzel, M. A Ga<sub>2</sub>O<sub>3</sub> Underlayer as an Isomorphic Template for Ultrathin Hematite Films toward Efficient Photoelectrochemical Water Splitting. *Faraday Discuss.* **2012**, *155*, 223.
- (17) Hisatomi, T.; Dotan, H.; Stefić, M.; Sivula, K.; Rothschild, A.; Grätzel, M.; Mathews, N. Enhancement in the Performance of Ultrathin Hematite Photoanode for Water Splitting by an Oxide Underlayer. *Adv. Mater.* **2012**, *24*, 2699–2702.
- (18) Warren, S. C.; Voitchovsky, K.; Dotan, H.; Leroy, C. M.; Cornuz, M.; Stellacci, F.; Hébert, C.; Rothschild, A.; Grätzel, M. Identifying Champion Nanostructures for Solar Water-Splitting. *Nat. Mater.* **2013**, *12*, 842–849.
- (19) Klahr, B.; Gimenez, S.; Fabregat-Santiago, F.; Hamann, T.; Bisquert, J. Water Oxidation at Hematite Photoelectrodes: The Role of Surface States. *J. Am. Chem. Soc.* **2012**, *134*, 4294–4302.
- (20) Klahr, B.; Gimenez, S.; Fabregat-Santiago, F.; Bisquert, J.; Hamann, T. W. Electrochemical and Photoelectrochemical Investigation of Water Oxidation with Hematite Electrodes. *Energy Environ. Sci.* **2012**, *5*, 7626.
- (21) Barroso, M.; Mesa, C. a; Pendlebury, S. R.; Cowan, A. J.; Hisatomi, T.; Sivula, K.; Grätzel, M.; Klug, D. R.; Durrant, J. R. Dynamics of Photogenerated Holes in Surface Modified  $\alpha$ -Fe<sub>2</sub>O<sub>3</sub> Photoanodes for Solar Water Splitting. *Proc. Natl. Acad. Sci. U. S. A.* **2012**, *109*, 15640–15645.
- (22) Barroso, M.; Pendlebury, S.; Cowan, A.; Durrant, J. Charge Carrier Trapping, Recombination and Transfer in Hematite ( $\alpha$ -Fe<sub>2</sub>O<sub>3</sub>) Water Splitting Photoanodes. *Chem. Sci.* **2013**, *4*, 2724.
- (23) Klahr, B. M.; Hamann, T. W. Current and Voltage Limiting Processes in Thin Film Hematite Electrodes. *J. Phys. Chem. C* **2011**, *115*, 8393–8399.
- (24) Dotan, H.; Sivula, K.; Grätzel, M.; Rothschild, A.; Warren, S. C. Probing the Photoelectrochemical Properties of Hematite ( $\alpha$ -Fe<sub>2</sub>O<sub>3</sub>) Electrodes Using Hydrogen Peroxide as a Hole Scavenger. *Energy Environ. Sci.* **2011**, *4*, 958.
- (25) Klahr, B.; Gimenez, S.; Fabregat-Santiago, F.; Bisquert, J.; Hamann, T. W. Photoelectrochemical and Impedance Spectroscopic

Investigation of Water Oxidation with “Co–Pi”-Coated Hematite Electrodes. *J. Am. Chem. Soc.* **2012**, *134*, 16693–16700.

(26) Zhong, D. K.; Gamelin, D. R. Photoelectrochemical Water Oxidation by Cobalt Catalyst (“Co–Pi”)/ $\alpha$ -Fe<sub>2</sub>O<sub>3</sub> Composite Photoanodes: Oxygen Evolution and Resolution of a Kinetic Bottleneck. *J. Am. Chem. Soc.* **2010**, *132*, 4202–4207.

(27) Kim, J. Y.; Magesh, G.; Youn, D. H.; Jang, J.-W.; Kubota, J.; Domen, K.; Lee, J. S. Single-Crystalline, Wormlike Hematite Photoanodes for Efficient Solar Water Splitting. *Sci. Rep.* **2013**, *3*, 1–8.

(28) Du, C.; Yang, X.; Mayer, M. T.; Hoyt, H.; Xie, J.; McMahon, G.; Bischooping, G.; Wang, D. Hematite-Based Water Splitting with Low Turn-On Voltages. *Angew. Chem., Int. Ed. Engl.* **2013**, *52*, 12692–12695.

(29) Lin, Y.; Zhou, S.; Sheehan, S. W.; Wang, D. Nanonet-Based Hematite Heteronanostructures for Efficient Solar Water Splitting. *J. Am. Chem. Soc.* **2011**, *133*, 2398–2401.

(30) Ling, Y.; Wang, G.; Wheeler, D. a.; Zhang, J. Z.; Li, Y. Sn-Doped Hematite Nanostructures for Photoelectrochemical Water Splitting. *Nano Lett.* **2011**, *11*, 2119–2125.

(31) Bohn, C. D.; Agrawal, A. K.; Walter, E. C.; Vaudin, M. D.; Herzing, A. A.; Haney, P. M.; Talin, A. A.; Szalai, V. A. Effect of Tin Doping on  $\alpha$ -Fe<sub>2</sub>O<sub>3</sub> Photoanodes for Water Splitting. *J. Phys. Chem. C* **2012**, *116*, 15290–15296.

(32) Hahn, N. T.; Mullins, C. B. Photoelectrochemical Performance of Nanostructured Ti- and Sn-Doped. *Chem. Mater.* **2010**, *22*, 6474–6482.

(33) Beermann, N.; Vayssieres, L.; Lindquist, S.-E.; Hagfeldt, A. Photoelectrochemical Studies of Oriented Nanorod Thin Films of Hematite. *J. Electrochem. Soc.* **2000**, *147*, 2456.

(34) Klahr, B. M.; Hamann, T. W. Voltage Dependent Photocurrent of Thin Film Hematite Electrodes. *Appl. Phys. Lett.* **2011**, *99*, 063508.

(35) Kronawitter, C. X.; Zegkinoglou, I.; Rogero, C.; Guo, J.-H.; Mao, S. S.; Himpel, F. J.; Vayssieres, L. On the Interfacial Electronic Structure Origin of Efficiency Enhancement in Hematite Photoanodes. *J. Phys. Chem. C* **2012**, *116*, 22780–22785.

(36) Barroso, M.; Cowan, A. J.; Pendlebury, S. R.; Grätzel, M.; Klug, D. R.; Durrant, J. R. The Role of Cobalt Phosphate in Enhancing the Photocatalytic Activity of  $\alpha$ -Fe<sub>2</sub>O<sub>3</sub> toward Water Oxidation. *J. Am. Chem. Soc.* **2011**, *133*, 14868–14871.

(37) Bard, A. J.; Bocarsly, A. B.; Fan, F. F.; Walton, E. G.; Wrighton, M. S. The Concept of Fermi Level Pinning at Semiconductor/Liquid Junctions. *J. Am. Chem. Soc.* **1980**, *102*, 3671.

(38) Lewerenz, H. J. Surface States and Fermi Level Pinning at Semiconductor/Electrolyte Junctions. *J. Electroanal. Chem.* **1993**, *356*, 121–143.

(39) Kanan, M. W.; Nocera, D. G. In Situ Formation of an Oxygen-Evolving Catalyst in Neutral Water Containing Phosphate and Co<sup>2+</sup>. *Science* **2008**, *321*, 1072–1075.